Chin. J. Astron. Astrophys. Vol. 6 (2006), No. 2, 227–236
(*http://www.chjaa.org*)

Chinese Journal of
Astronomy and
Astrophysics

A Non-axisymmetric Spherical α^2-Dynamo *

Jie Jiang and Jing-Xiu Wang

National Astronomical Observatories, Chinese Academy of Sciences, Beijing 100012;
jiangjie@ourstar.bao.ac.cn

Received 2005 July 28; accepted 2005 September 20

Abstract Using the Chebyshev-tau method, the generation of oscillatory non-axisymmetric stellar magnetic fields by the α^2-dynamo is studied in spherical geometry. Following the boundary conditions given by Schubert & Zhang, the spherical α^2-dynamo consists of a fully convective spherical shell with inner radius r_i and outer radius r_o. A comparison of the critical dynamo numbers of axisymmetric and ϕ-dependent modes for different thicknesses of the convective shell and different α-profiles leads to the following qualitative results: (i) when the angular factor of α-profile is $\sin^n\theta\cos\theta$ ($n = 1, 2, 4$) the solutions of the α^2-dynamo are oscillatory and non-axisymmetric, (ii) the thinner the convective shell, the more easily is the non-axisymmetric mode excited and the higher is the latitudinal wave number, (iii) the thickness of the outer convective shell has an effect on the symmetries of the magnetic fields.

Key words: stars: magnetic fields — methods: numerical

1 INTRODUCTION

A dynamo process is recognized to explain the cyclic evolution of stellar magnetic fields in which two basic processes are involved. The first one is Ω-effect which shears pre-existing poloidal fields by differential rotation to produce a relatively strong toroidal fields; the second is α-effect which lifts and twists toroidal flux tubes to regenerate poloidal fields (Parker 2001). Combination of the two mechanisms at different relative magnitudes leads to three types of turbulent dynamo: α^2-dynamo, $\alpha^2\Omega$-dynamo and $\alpha\Omega$-dynamo (Hoyng 1991).

However, both observations and theories indicate that during the evolution of typical magnetic stars of spectral Type A or F, they pass through a fully convective Hayashi phase, and there are some pre-main sequence (T Tauri, M dwarf, etc.) stars which are fully convective objects. For these stars the type of dynamo is α^2-dynamo produced only by the α effect.

Traditional solution of α^2-dynamo is stationary and axisymmetric (Krause & Rädler 1980). The oscillatory dynamo behavior is produced by a combination of the α-effect and differential rotation. Cyclic variations of such activity indicators as area covered by photospheric spots, spots latitudes and longitudes, strength of chromospheric emission lines, are expected to occur on active stars (Cutispoto & Rodonó 1992). There have been pioneer works done in the search for oscillatory solutions of α^2-dynamo. Baryshnikova & Shukurov (1987) discussed a one dimensional α^2-dynamo in a thin disc of turbulent conducting fluid and demonstrated that oscillatory magnetic fields can be

* Supported by the National Natural Science Foundation of China.

generated. These oscillations were suggested to be generated by boundary effects; Rädler & Bräuer (1987) investigated axisymmetric spherical and disk models for pure α^2-dynamo and pointed out that the oscillations depended on the gradient of α.

Furthermore, observations of starspot distribution obtained by Doppler imaging showed non-axisymmetric patterns of magnetic fields (Piskunov et al. 1990) in equatorial and high-latitude spots (Hatzes 1995; Rice & Strassmeier 1996), and gave little indications of magnetic dipole field geometry in T Tauri stars (Joncour et al. 1994). The famous non-axisymmetric feature, i.e., the flip-flop phenomenon, occurs not only on the surface of rapidly rotating late-type giants FK Com and RS CVn (Berdyugina & Tuominen 1998) but also in single young dwarfs (Rice & Strassmeier 1998). Therefore, further work is desirable to seek after non-axisymmetric and oscillatory dynamo solutions of the α^2-dynamo.

Rüdiger & Elstner (1994) concluded that, in the absence of differential rotation, when α-tensor is highly anisotropic and its azimuthal component dominates over all the other components, non-axisymmetric magnetic modes would be preferred. Moss et al. (1991) and Küker & Rüdiger (1999) solved the nonlinear induction equation in three dimensions and found stable non-axisymmetric solutions. Schubert & Zhang (2000) reported that oscillatory α^2-dynamo behavior occurs when the outer region of the dynamo action surrounds a large, less magnetically diffusive core. The solutions were non-axisymmetric and expanded in terms of spherical harmonics $P_l^m(\cos\theta)\mathrm{e}^{\mathrm{i}m\phi}$. Since only the simplest case of a constant α was considered, the spherical harmonics were decoupled and only the lowest order (l=1) was discussed by them. Rüdiger et al. (2003) showed the basic solution for α^2-dynamo was non-axisymmetric and always of quadrupolar parity when the α-effect is latitudinally inhomogeneous and anisotropic. However, only the first non-axisymmetric modes ($m = 1$) were considered.

In the present paper, the generation of oscillatory non-axisymmetric stellar magnetic fields is examined for the α^2-dynamo by using the Chebyshev-tau method. Both the toroidal and poloidal magnetic fields are expanded in terms of Chebyshev functions for the radial dependence and spherical harmonic functions for the angular dependence. The easiest excited modes are sought at the onset of dynamo action for different thicknesses of the convective zone and different α-profiles. The method is checked by analytic solutions with a simple α-profile. We attempted to answer the following questions: (i) how do different α-profiles affect the spherical geometry of the dynamo action?, (ii) can a spherical α^2-dynamo generate a non-axisymmetric and oscillatory magnetic fields? and (iii) what determines the equatorial symmetry of a spherical dynamo? The basic equations are considered in Section 2. The numerical scheme is described in Section 3. We discuss our results in Section 4 and give a summary in Section 5.

2 BASIC EQUATIONS OF OUR MODEL

Our model consists of a turbulent fluid spherical shell of inner radius r_i surrounding a perfect inducting radiative core and outer radius r_o surrounded by insulator (vacuum). We use the usual spherical polar coordinates (r, θ, ϕ) (see Fig. 1). The starting point of our model is the mean-field dynamo equation without a flow field, governing the evolution of the large scale magnetic fields in response to the α-effect and magnetic diffusivity,

$$\frac{\partial \boldsymbol{B}}{\partial t} = \nabla \times (\alpha \boldsymbol{B}) - \nabla \times (\beta \nabla \times \boldsymbol{B}), \tag{1}$$

where $\boldsymbol{B}$ is the mean magnetic field, β is the turbulent magnetic diffusivity. Since the anisotropic β seems not strong (Kitchatinov 2002), we regard it as a constant. The overall structure of α is a tensor and it represents the interaction of the anisotropic turbulence with the global rotation and the magnetic fields. In order to simplify our model we use the following scalar expression for the α-profile in which the nonlinear effect such as α-quenching is neglected,

$$\alpha = \alpha_0 f(r,\theta), \qquad f(r,\theta) = \sin^n\theta\cos\theta\sin\left[\frac{r-r_i}{r_\mathrm{o}-r_i}\right], \tag{2}$$

where α_0 is the scale of the α-effect with the dimension of a velocity. The angular factor $\cos\theta$ comes from the angular dependence of Coriolis force. Here n is an adjustable parameter. The

introduction of $\sin^n\theta$ guarantees the α-effect to have a distribution in latitude that is weak in the polar area. The larger n is, the more the magnetic fields concentrate to the equator (see Fig. 2). The r dependence of α satisfies $\alpha(r_i,\theta)=\alpha(r_o,\theta)=0$.

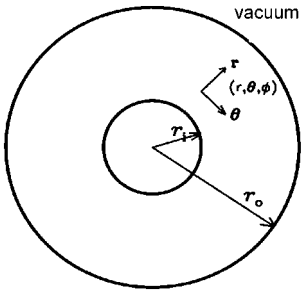

Fig. 1 Geometry of the non-axisymmetric spherical dynamo in a meridional plane. Its inner radius is r_i and outer radius r_o. The radiative core ($r<r_i$) is a perfect electrical insulator, outside of the shell ($r>r_o$) is vacuum and the magnetic field is potential.

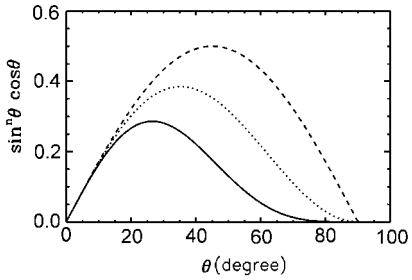

Fig. 2 Angular dependence of α-profile $\sin^n\theta\cos\theta$ for different n. The solid line corresponds to $n=4$, dashed line to $n=2$, dotted line to $n=1$. The larger n is, the more is the α-effect concentrated toward the equator.

We de-dimension length by the thickness of the shell r_o-r_i and time by the magnetic diffusion time $\frac{(r_o-r_i)^2}{\beta}$, then Equation (1) becomes

$$\frac{\partial \boldsymbol{B}}{\partial t}=R_\alpha\nabla\times(f\,(r,\theta)\boldsymbol{B})+\nabla^2\boldsymbol{B}, \tag{3}$$

where $R_\alpha=\frac{\alpha_0(r_o-r_i)}{\beta}$ is the magnetic Reynolds number, an important parameter in the dynamo calculation that measures the relative importance of the α-effect to the diffusive effect. Since the magnetic field is divergence-free, we expand $\boldsymbol{B}$ in term of two scalar functions, h and g, which represent the poloidal and toroidal potentials, respectively (Chandrasekhar 1961; Moffat 1978; Zhang & Liao 2003)

$$\boldsymbol{B}=\nabla\times\nabla\times\boldsymbol{r}h(r,\theta,\phi,t)+\nabla\times\boldsymbol{r}g(r,\theta,\phi,t), \tag{4}$$

where $\boldsymbol{r}\cdot\boldsymbol{B}=L^2h$, $\boldsymbol{r}\cdot(\nabla\times\boldsymbol{B})=L^2g$, $L^2=-\frac{1}{\sin\theta}\frac{\partial}{\partial\theta}\sin\theta\frac{\partial}{\partial\theta}-\frac{1}{\sin^2}\frac{\partial}{\partial\phi^2}$.

The equations for the poloidal and toroidal field components can be obtained by applying $\boldsymbol{r}\cdot$ and $\boldsymbol{r}\cdot\nabla\times$ to Equation (3). Thus,

$$\frac{\partial}{\partial t}L^2h=R_\alpha\Big(\frac{\partial f}{\partial\theta}B_\phi+f\,L^2g\Big)+L^2\nabla^2h, \tag{5}$$

$$\frac{\partial}{\partial t}L^2g=R_\alpha\Big[\frac{1}{r}\frac{\partial}{\partial r}\Big(r\frac{\partial f}{\partial r}\Big)L^2h+\frac{\partial^2 f}{\partial r\partial\theta}B_\theta-(\nabla L^2h)\cdot\nabla f-L^2h\nabla^2f+\frac{\partial f}{\partial\theta}(\nabla\times B\,)_\phi-f\,\nabla^2L^2h\,\Big]+L^2\nabla^2g, \tag{6}$$

where $B_\phi=\frac{1}{r\sin\theta}\frac{\partial h}{\partial\phi}+\frac{1}{\sin\theta}\frac{\partial^2h}{\partial r\partial\phi}-\frac{\partial g}{\partial\theta}$, $B_\theta=\frac{1}{\sin\theta}\frac{\partial g}{\partial\phi}+\frac{1}{r}\frac{\partial h}{\partial\theta}+\frac{\partial^2 g}{\partial r\partial\theta}$,

$$(\nabla\times\boldsymbol{B})_\phi=\frac{\partial}{\partial\theta}\nabla^2h+\frac{1}{r}\frac{1}{\sin\theta}\frac{\partial g}{\partial\phi}+\frac{1}{\sin\theta}\frac{\partial^2 g}{\partial r\partial\phi},\qquad \nabla^2=\frac{1}{r^2}\frac{\partial}{\partial r}r^2\frac{\partial}{\partial r}-\frac{1}{r^2}L^2.$$

For the radial component B_r, it is equal to L^2h/r.

As is well known, boundary conditions play an important role in the solution of hydromagnetic equations (see the discussion in Schubert & Zhang 2001). In the present paper, the boundary conditions at $r=r_o$ and $r=r_i$ for Equations (5) and (6) are straightforward. We assume the radiative core ($r<r_i$) to behave effectively as a perfectly conducting inner core. The exterior

($r > r_o$) is a vacuum and the magnetic field is assumed to be potential. Since both the magnetic fields and tangential electric fields must be continuous at the two interfaces (Schubert & Zhang 2001; Ossendrijver 2003), we obtain

$$\text{at} \quad r = r_i, \qquad h(r_i) = 0, \qquad -R_\alpha r_i f(r,\theta)\frac{\partial h}{\partial r} + \frac{\partial (rg)}{\partial r} = 0, \tag{7}$$

$$\text{at} \quad r = r_o, \qquad g(r_o) = 0, \qquad r_o \frac{\partial h}{\partial r} + (1+l)h = 0, \tag{8}$$

where l comes from the Legendre function P_l^m which is the expansion of the latitude dependence of h and g (see Schubert & Zhang 2001 for details).

3 NUMERICAL SCHEME

Since the dynamo equations, Eqs. (5) and (6), are two coupled, linear homogeneous equations in h and g, we can look for their eigen solutions in the form of

$$[h(r,\theta,\phi), g(r,\theta,\phi)] = [h(r,\theta,\phi), g(r,\theta,\phi)]\mathrm{e}^{st}, \tag{9}$$

where s is the generally complex eigenvalue, $s = \sigma + i\omega$. Real s means monotonic time-dependence and complex s indicates oscillation. The real part of s gives the growth rate and its imaginary part, ω, provides the frequency of the oscillatory mode. If the imaginary part of s is zero, the kinematic dynamo is stationary.

According to the Chebyshev-tau method, we expand $h(r,\theta,\phi)$ and $g(r,\theta,\phi)$ in terms of Chebyshev polynomials $T_n(\hat{\boldsymbol{r}})$ and surface harmonics $P_l^m \mathrm{e}^{\mathrm{i}m\phi}$ in the meridional circular sector $r \in [r_i, r_o]$, $\theta \in [0,\pi]$, where θ is the co-latitude and $\hat{\boldsymbol{r}}$ range from –1 to 1. The numerical solution is fully resolved in r and θ, but is severely truncated in ϕ so that a single value of m is given. We have

$$h = \sum_{n=0}^{\infty}\sum_{l=m}^{\infty} c_{n,l}^h T_n(\hat{\boldsymbol{r}}) P_l^m(\cos\theta)\mathrm{e}^{\mathrm{i}m\phi}, \tag{10}$$

and

$$g = \sum_{n=0}^{\infty}\sum_{l=m}^{\infty} c_{n,l}^g T_n(\hat{\boldsymbol{r}}) P_l^m(\cos\theta)\mathrm{e}^{\mathrm{i}m\phi}, \tag{11}$$

where $\hat{\boldsymbol{r}} = 2r - \frac{1+\eta}{1-\eta} \in [-1,+1]$, η is the ratio of r_i/r_o and m is the azimuthal wave number. If $m \neq 0$, the solution corresponds to a non-axisymmetric mode. In contrast to the axisymmetric mode ($m = 0$), the non-axisymmetric mode has the form of a wave propagating along the azimuth (the $\cos(\omega t - m\phi)$ type wave) (Ivanova & Ruzmaikin 1985). Here $c_{n,l}^h$ and $c_{n,l}^g$ are the eigenvectors and are complex in general. Equations (5) and (6) can be expanded in terms of Equations (10) and (11) based on $L^2 Y_l^m = l(l+1)Y_l^m$. As to the four boundary conditions, they can be expressed according to Equations (7), (8), (10) and (11) in detail as follows.

$$\sum_{n=0}^{\infty}\sum_{l=0}^{\infty} c_{n,l}^h (-1)^n P_l^m(\cos\theta) = 0, \tag{12}$$

$$\sum_{n=0}^{\infty}\sum_{l=0}^{\infty} c_{n,l}^h [2(-1)^{n+1} n^2 r_i + (-1)^n] P_l^m(\cos\theta) = 0 \quad \text{at} \quad r = r_i, \tag{13}$$

$$\sum_{n=0}^{\infty}\sum_{l=0}^{\infty} c_{n,l}^g P_l^m(\cos\theta) = 0, \tag{14}$$

$$\sum_{n=0}^{\infty}\sum_{l=0}^{\infty} c_{n,l}^h [2n^2 r_o + (1+l)] P_l^m(\cos\theta) = 0 \qquad \text{at} \quad r = r_o. \tag{15}$$

After truncating the infinite set of equations at $n = n_{\max}$ and $l = l_{\max}$, a finite system is obtained. We set up a numerical scheme to determine the eigenvalues s and eigenvectors $c^h_{n,l}, c^g_{n,l}$. In general, if $n > n_{\max}$ and $l > l_{\max}$, the eigenvalues apparently converge, $n_{\max}$ and $l_{\max}$ are different for different model parameters. We seek the eigenvalues of Equations (5) and (6) for each given m, i.e. we consider separately the evolution of each ϕ harmonic of the magnetic fields because $\boldsymbol{B}$ is linear and the profile of α is axisymmetric (Ivanova & Ruzmaikin 1985). We consider only those modes that neither grow nor decay, with the real part of s zero. The corresponding magnetic Reynolds number R_α is the critical dynamo number $R_{\alpha_{cr}}$, which we also denote by R_α in the following for simplicity. Each mode has its own critical dynamo number. The mode with the lowest critical dynamo number is the preferred stable mode (Krause & Meinel 1988).

As pointed out by Ivanova & Ruzmaikin (1985), with boundary conditions (Eqs.(7) and (8)), the system of Equations (5) and (6) can be decomposed into two subsystems. One is $c^h_{n,l}$ with l odd $(c^h_{n,1}, c^h_{n,3}, c^h_{n,5} \cdots\cdots)$ and $c^g_{n,l}$ with l even $(c^g_{n,0}, c^g_{n,2}, c^g_{n,4} \cdots\cdots)$. The other is $c^h_{n,l}$ with l even and $c^g_{n,l}$ with l odd. According to the symmetry of adjoint Legendre polynomial, if m is odd, the first subsystem generates the magnetic fields with a radial component B_r that is symmetric with respect to the equatorial plane $(\theta \to \pi - \theta)$ and B_θ is antisymmetric and B_ϕ is symmetric . It is the so called "quadrupole parity" solution, and we label it as S. The second subsystem generates the antisymmetric B_r, symmetric B_θ and antisymmetric B_ϕ, i.e., "dipole parity" solution, labelled as A.

4 RESULTS

We first discuss the simple profile with $\alpha =$ constant, i.e. $f(r, \theta) = 1$ as a test of our numerical scheme with analytical results and then carry out an investigation of the characters of the α^2-dynamo.

4.1 Dynamo for Constant α-Profile

When $\alpha =$ constant, Equations (5) and (6) reduce to

$$(\nabla^2 - s)L^2 h + R_\alpha L^2 g = 0, \tag{16}$$

$$(\nabla^2 - s)L^2 g - R_\alpha L^2 \nabla^2 h = 0, \tag{17}$$

where $\partial/\partial t$ is replaced by s, and h and g are independent. The exact solution to Equations (16) and (17) is

$$h = [a_1 j_l(\xi_1 r) + b_1 n_l(\xi_1 r) + a_2 j_l(\xi_2 r) + b_2 n_l(\xi_2 r)] Y^m_l(\theta, \phi) \mathrm{e}^{st}, \tag{18}$$

$$g = \left\{ \frac{\xi_1^2 + s}{R_\alpha} [a_1 j_l(\xi_1 r) + b_1 n_l(\xi_1 r)] + \frac{\xi_2^2 + s}{R_\alpha} [a_2 j_l(\xi_2 r) + b_2 n_l(\xi_2 r)] \right\} Y^m_l(\theta, \phi) \mathrm{e}^{st}, \tag{19}$$

where $j_l(r)$ and $n_l(r)$ are spherical Bessel functions of the first and second kinds, respectively, and $\xi_1 = \frac{1}{2}[R_\alpha + \sqrt{R_\alpha^2 - 4s}]$, $\xi_2 = \frac{1}{2}[R_\alpha - \sqrt{R_\alpha^2 - 4s}]$. For each mode m, exact analytic expression for h and g in this case can be found according to the determinant of a 4×4 matrix obtained from substituting Equations (18) and (19) into the four boundary conditions. Because the α-profile is constant, the spherical harmonics in the solutions of equations (16) and (17) are decoupled. It is convenient to discuss the lowest order ($l = 1$). We obtained the eigenvalues also by the numerical method mentioned above. The dynamo number R_α is adjusted until onset of dynamo action takes place (i.e., the real part of the eigenvalue s is near to zero). With the critical dynamo number R_α given by numerical method, we can find the analytical growth rate s by the dispersion relation, $\mathrm{Det}[c_{i,j}(R_\alpha, s)] = 0$.

Table 1 shows the numerical result s^{num} and the analytical result s^{exa} for different $r_i/r_{\mathrm{o}}\,(\eta)$ ratios. The real parts of all s in Table 1 are less than 10^{-3} (not shown in the table), so they correspond to the onset of the dynamo action. The agreement between exact and numerical solutions is better than 0.1% and the results, $\eta = 0.6$ and $\eta = 0.8$, are the same as the corresponding parts in Schubert & Zhang (2001).

Table 1 Exact solutions $s^{\rm exa}$ and numerical ones $s^{\rm num}$ and the corresponding dynamo number R_α for constant α-profile with the lowest order ($l = 1$). The agreement between them is better than 0.1%.

η	$R_\alpha^{\rm exa}$	$s^{\rm exa}$	$R_\alpha^{\rm num}$	$s^{\rm num}$
0.4	4.78	i1.319	4.78	i1.319
0.6	4.38	i2.979	4.38	i2.979
0.8	4.14	i3.358	4.14	i3.358

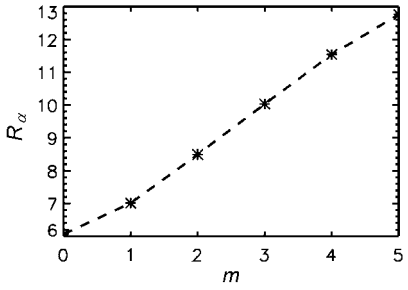

Fig. 3 Dynamo number R_α for modes $m = 0 - 5$ with $r_i/r_{\rm o} = 0.4$ for latitudinally inhomogeneous α-effect ($\alpha \sim \cos\theta \sin[\pi \frac{r-r_i}{r_{\rm o}-r_i}]$). The axisymmetric mode $m = 0$ is the stable mode.

Table 2 Dynamo numbers R_α and frequencies ω for modes $m = 0 - 4$ with different ratios of $r_i/r_{\rm o}$ (η).

η	$m = 0$	$m = 1$	$m = 2$	$m = 3$	$m = 4$
0.4	R_α=6.06, ω=0	R_α=7.01, ω=0	R_α= 8.49, ω=0	R_α=10.03, ω=0	R_α=11.62, ω=0
0.6	R_α=5.60, ω=0	R_α=6.09, ω=0	R_α=6.71, ω=0	R_α=7.476, ω=0	R_α=8.311, ω=0
0.8	R_α=5.38, ω=0	R_α=5.51, ω=0	R_α=5.71, ω=0	R_α=5.798, ω=0	R_α=6.025, ω=0

4.2 Latitudinally Inhomogeneous α-effect ($\alpha \sim \cos\theta \sin[\pi \frac{r-r_i}{r_{\rm o}-r_i}]$)

We adopt the angular dependence of α-effect as $\cos\theta$, being the simplest form of antisymmetry across the equatorial plane. The radial dependence satisfies $\alpha = 0$ at the two interfaces $r = r_{\rm o}$ and $r = r_i$, and the maximal value of α occurs at the halfway point of the spherical shell. For a giving m, when $n_{\max}$ and $l_{\max} - m$ are larger than 12 in Equations (10) and (11), all the eigenvalues will converge. We first take $r_i/r_{\rm o} = 0.4$ for a test. Figure 3 shows the dynamo numbers R_α for different modes. As m increases, the dynamo number R_α increases too. The axisymmetric mode ($m = 0$) corresponds to the lowest R_α. Calculations for other ratios of $r_i/r_{\rm o}$ give the same trend (seen Table 2). Since the mode with the lowest dynamo number is the preferred stable mode (Krause & Meinel 1988), we say all the solutions with this simply α-profile are axisymmetric. Furthermore, the imaginary parts of the eigenvalues s, i.e., the frequency ω, are zero. So all the modes are stationary. So we conclude, just as in the conventional wisdom on α^2-dynamo solution, all the modes are stationary and axisymmetric. We note that R_α decreases with increasing $r_i/r_{\rm o}$ ratio, that is, the thinner the shell is, the easier is the axisymmetric mode excited.

4.3 Latitudinally Inhomogeneous α-effect ($\alpha \sim \sin^2\theta \cos\theta \sin[\pi \frac{r-r_i}{r_{\rm o}-r_i}]$)

In this subsection we adopt the profile, $\sin^2\theta \cos\theta \sin[\pi \frac{r-r_i}{r_{\rm o}-r_i}]$. Figure 4 displays the values of the dynamo number R_α for the modes $m = 1 - 4$, separately for two values of of the ratio r_i to $r_{\rm o}$, 0.4

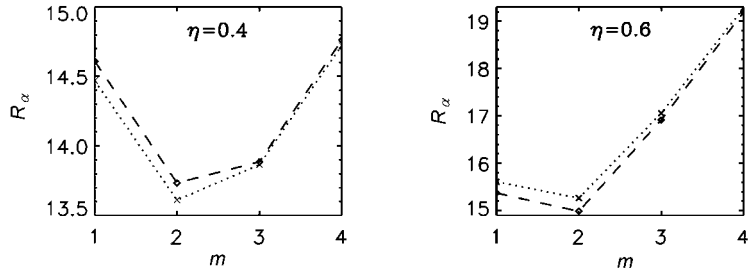

Fig. 4 Dynamo number R_α for latitudinally inhomogeneous α-effect profile ($\alpha \sim \cos\theta \sin^2\theta \sin[\pi \frac{r-r_i}{r_o-r_i}]$) for r_i/r_o ratio of 0.4 (left) and 0.6 (right). The dashed line links the symmetric solutions and the dotted line, the anti-symmetric ones with respect to the equatorial plane.

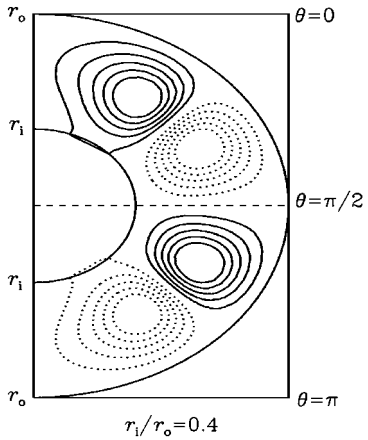

Fig. 5 Contours of the toroidal field B_ϕ in a meridional plane for the $\alpha \sim \sin^2\theta\cos\theta \sin[\pi\frac{r-r_i}{r_o-r_i}]$ profile, R_α=14.986 and r_i/r_o=0.4 at t=0. Dashed contours indicate for $B_\phi < 0$, and solid contours for $B_\phi > 0$. The field is anti-symmetric with respect to the equatorial plane.

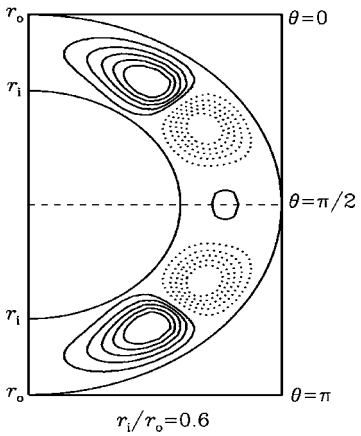

Fig. 6 Contours of the toroidal field B_ϕ in a meridional plane for the $\alpha \sim \sin^2\theta\cos\theta \sin[\pi\frac{r-r_i}{r_o-r_i}]$ profile, R_α=13.61 and r_i/r_o=0.6 at t=0. Dashed contours indicate for $B_\phi < 0$, and solid contours for $B_\phi > 0$. The toroidal fields are symmetric with respect to the equatorial plane.

and 0.6. The dashed line links the quadrupole parity solutions and the dotted line, the dipole parity solutions. When $r_i/r_o = 0.4$ the dipole parity solutions lie somewhat lower than the quadrupole parity solutions, the latter are excited somewhat more easily than the former. The second harmonic m=2 corresponds to a minimum R_α (we only check the modes 0–5, which could be enough). Thus, the solution for the model with α-profile $\sin^2\theta\cos\theta\sin[\pi\frac{r-r_i}{r_o-r_i}]$ and r_i/r_o=0.4 is non-axisymmetric with azimuthal wavenumber m=2. For the poloidal fields, $C^h_{n,3}$ and $C^h_{n,5}$ are much larger than the other coefficient of $C^h_{n,l}$ according to the eigenvector, and the latitudinal distribution of B_r is mainly dominated by the adjoint Legendre polynomials P_3^2 and P_5^2. Moreover, P_2^2 and P_4^2 are dominant for the toroidal magnetic fields. So, B_r is symmetric with respect to the equatorial plane, B_θ is antisymmetric and B_ϕ is symmetric. So the fields have "dipole parity". Figure 5 presents the B_ϕ contour which is anti-symmetric respect to the equatorial plane in a meridional plane at t=0. For this stable anti-symmetric mode, the imaginary part of s is 0.2198. Given the values of the magnetic diffusion β and the radius of the stellar radius, we can obtain the star's magnetic cycle. The variation of the total magnetic field energy is cyclic too.

The right panel of Figure 4 shows the case of $r_i/r_o = 0.6$. Contrary to the case of r_i/r_o=0.4, R_α for the quadrupole parity solutions are to some extent lower than the dipole parity ones. So in this case the quadrupole parity solutions are more easily excited. The solution for this model is oscillatory with non-axisymmetric mode m=2 too. However, because the adjoint Legendre polynomials P_2^2 and P_2^4 dominate the poloidal field, and P_3^2 and P_5^2, the toroidal field, the field is symmetric respect to the equatorial plane. Figure 6 shows the corresponding B_ϕ contours in a meridional plane at t=0.

To sum up, when we adopt the α-profile $\sin^2\theta\cos\theta\sin[\pi\frac{r-r_i}{r_o-r_i}]$, all the solutions are oscillatory and non-axisymmetric. Whether the dipolar or quadrupole parity solutions are excited depends on the ratio of r_i/r_o. When the convective shell is thin the symmetric solutions are easier to be excited. Otherwise the anti-symmetry ones will be excited. This conclusion will be further clarified in the following subsection.

4.4 Results from Varying n and r_i/r_o

In the following, we shall discuss the equatorial antisymmetric α-profile $\sin^n\theta\cos\theta\sin[\pi\frac{r-r_i}{r_o-r_i}]$ with n=1, 2 or 4, describing the latitudinal profile of the α-effect. The term $\sin^n\theta$ plays an essential role in producing non-axisymmetric oscillatory solutions. We investigate the solutions for the profile with different values of n and r_i/r_o with the numerical method mentioned in Section 3. Tables 3–5 list the results for the critical dynamo number R_α and the frequency ω for the different parameter values. Here Am denotes a solution that is anti-symmetric with respect to the equatorial plane (dipolar parity solution) and with azimuthal wave number m, while Sm denotes a symmetric solution (quadrupole parity solution).

Tables 3, 4 and 5 show that with the $\sin^n\theta$ dependence, we obtain the same conclusion as in Subsection 4.3, i.e., all of them have non-axisymmetric oscillatory solutions. Although the oscillatory axisymmeric solutions may occur in our test, they do not correspond to the lowest dynamo numbers. We try to find the most easily excited mode for different n and different η. Comparing results for different ratios of inner radius to outer radius (η = 0.2, 0.4, 0.6 and 0.8) for the same parameter n in each of the three tables, it is obvious that as η increases, i.e., as the thickness of the shell decreases, the critical dynamo numbers R_α decreases and the mode number m that are the most easily excited increases. So, we have obtained the same conclusion as Rüdiger et al. (2003): "The thinner the (outer) α-shell, the higher is the latitudinal mode number m of the modes excited with the lowest dynamo number R_α." On the other hand, all the critical dynamo numbers R_α corresponding to dipole parity solutions are smaller than the quadrupole parity ones for η=0.2 and η=0.4. For η=0.6 and η=0.8, however, we have the contrary result. So we can conclude that when a $\sin^n\theta$ factor is included in the α-profile, all the solutions are oscillatory and non-axisymmetric. Whether the solutions are symmetric or anti-symmetric respect to the equatorial plane depends on the thickness of the convective shell. Further computation indicates that when the convective shell is relative thick ($r_i/r_o < 0.56$) the anti-symmetric solutions are somewhat more easily excited, and that, when the convective shell is thin ($0.56 < r_i/r_o < 1$) the symmetric ones are dominant.

5 CONCLUSIONS AND DISCUSSION

In this paper, we have investigated the characteristics of linear kinematic spherical α^2-dynamo. With the boundary conditions given by Schubert & Zhang(2001), we use Cheyshev-tau method to find the solutions of the dynamo equation, for which the radial dependence of the poloidal and toroidal magnetic fields is expanded in terms of the Chebyshev function $T_n(\hat{\boldsymbol{r}})$ and the angular dependence in terms of spherical harmonic $Y_l^m(\theta,\phi)$. It does not need much computation time and the convergence is fast. Another merit of the method is that the characteristic parameters of all the azimuthal modes, m=0, 1, 2 and 3 $\cdots$, for certain parameters can be sought and the modes that are the most easily excited can be identified. The code has been checked by the analytic solution with the simplest α-profile that is decoupled for each mode. Other numerical method to solve the eigenvalue problem has also been used to test the code. It is found they give consistent results.

Our calculation indicated that if the angular dependence of α is simply taken as $\cos\theta$ (the effect mainly concentrated in the polar area), the solution is stationary and axisymmetric, just

Table 3 Dynamo number R_α and the frequency ω of symmetric (S) and anti-symmetric (A) solutions $\alpha \sim \sin\theta\cos\theta\sin[\pi\frac{r-r_i}{r_o-r_i}]$ profile for four values of η=r_i/r_o, 0.2, 0.4, 0.6 and 0.8. The number following S or A is the mode number of the most easily excited mode.

$\eta = 0.2$		$\eta = 0.4$		$\eta = 0.6$		$\eta = 0.8$	
$(S1)R_\alpha$	ω	$(S1)R_\alpha$	ω	$(S2)R_\alpha$	ω	$(S5)R_\alpha$	ω
13.29	0.749	11.68	0.069	10.52	0.135	10.228	0.09
$(A1)R_\alpha$	ω	$(A1)R_\alpha$	ω	$(A2)R_\alpha$	ω	$(A5)R_\alpha$	ω
13.048	0.233	11.61	0.338	10.567	0.074	10.228	0.09

Table 4 The same as Table 3 but for the profile $\alpha \sim \sin^2\theta\cos\theta\sin[\pi\frac{r-r_i}{r_o-r_i}]$

$\eta = 0.2$		$\eta = 0.4$		$\eta = 0.6$		$\eta = 0.8$	
$(S1)R_\alpha$	ω	$(S2)R_\alpha$	ω	$(S2)R_\alpha$	ω	$(S4)R_\alpha$	ω
17.68	0.587	15.265	0.119	13.61	0.387	13.60	0.546
$(A1)R_\alpha$	ω	$(A2)R_\alpha$	ω	$(A2)R_\alpha$	ω	$(A4)R_\alpha$	ω
17.124	0.163	14.986	0.219	13.734	0.241	13.60	0.546

Table 5 The same as Table 3 but for the profile $\alpha \sim \sin^4\theta\cos\theta\sin[\pi\frac{r-r_i}{r_o-r_i}]$

$\eta = 0.2$		$\eta = 0.4$		$\eta = 0.6$		$\eta = 0.8$	
$(S2)R_\alpha$	ω	$(S2)R_\alpha$	ω	$(S3)R_\alpha$	ω	$(S5)R_\alpha$	ω
25.25	0.509	20.76	0.099	18.456	0.106	18.275	0.459
$(A2)R_\alpha$	ω	$(A2)R_\alpha$	ω	$(A3)R_\alpha$	ω	$(A5)R_\alpha$	ω
24.642	0.25	20.014	0.206	18.65	0.154	18.29	0.457

as in the traditional solution of α^2-dynamo. However, if we apply different angular α-dependence $\sin^n\theta\cos\theta\sin[\pi\frac{r-r_i}{r_o-r_i}]$ with n a positive integer (concentrating the α-effect closer to the equator), different results will be obtained. The eigenvalues and the corresponding critical dynamo numbers R_α for different ratios r_i/r_o can be summed up as follows. First, all the solutions are oscillatory and non-axisymmetric; secondly, the thinner the convective shell is, the easier are the non-axisymmetric modes excited and the higher is the azimuthal wave number; thirdly, for n not equal to zero, the smaller n is, the more easily are the non-axisymmetric modes excited; fourthly, whether the solution is symmetric or anti-symmetric respect to the equatorial plane depends on the thickness of the convective shell: if the core is large enough ($> 0.56r_o$), the solution is almost symmetric, but if it is smaller than $0.56r_o$, it will be of anti-symmetric.

The results are useful for explaining some observed features of some of the fully convective stars listed in Section 1, such as the cyclical variation of magnetic activities, non-axisymmetric patterns of the magnetic fields and non-dipole field geometry in T Tauri stars. They maybe also apply to earth and the planets.

The inclusion of angular dependence α-profile $\sin^n\theta$ plays an important role in finding non-axisymmetric and oscillatory solutions. However, the box simulations do not prove an angular dependence that deviated from the $\cos\theta$-law (Ossendrijver et al. 2001). So it may be only of academic interest (Rüdiger et al. 2003) and is introduced artificially to reduce the strength of the toroidal field at high latitudes (Chatterjee et al. 2004) although several authors have adopted it, e.g., Dikpati & Charbonneau(1999) used the angular factor $\sin\theta\cos\theta$, while Küker et al. (2001) and Chan et al. (2004) used $\sin^2\theta\cos\theta$. However, it may be reasonable to deduce the α-effect in the polar area, and we can obtain a non-axisymmetric and oscillatory solution for such α-profiles.

It seems too early to apply the solution to the observed stellar magnetic fields. However, the present approach does shed some light on understanding stellar magnetism. The relative thickness of convective zone and the α-dependence on the latitudes appear to be the key factors in

determining the behavior of stellar dynamo. Further studies will be undertaken, Particularly, by taking α as a tensor and by considering only the $\alpha_{\phi\phi}$-component in spherical coordinate in this paper, we may have lost some information. In this paper we neglected the differential rotation, but for checking what value the inverse Rossby number will reach the differential rotation must be taken into account. Also, what different actions will occur in different models? All of these will be included in our further work.

Acknowledgements We thank Prof. Xinhao Liao and Prof. Keke Zhang for their great help in connection with this work. We extend our thanks to Arnab Rai Choudhuri and Jun Zhang for reviewing the manuscript. This work is supported by the National Natural Science Foundation of China (G10573025) and by the National Key Basic Research Science Foundation (G2000078404). We thank the referee for very valuable comments and suggestions.

References

Baryshnikov Y., Shukurov A., 1987, Astron. Nachr., 308, 89
Berdyugina S. V., Tuominen I., 1998, A&A, 336, L25
Chan K. H., Zhang K., Zou J., Schubert G., 2001, Physics of the Earth and Planetary Interiors, 128, 35
Chandrasekhar S., 1961, Hydrodynamic and Hydromagnetic Stability, Oxford: Clarendon
Charbonneau P., Macgregor K. B., 2001, ApJ, 559, 1094
Chatterjee P., Nandy D., Choudhuri A. R., 2004, A&A, 427, 1019
Cutispoto G., Rodonó M., 1992, In: K. L. Harvey, ed., ASP Conf. Ser. Vol. 27, The Solar Cycke., San Francisco: ASP, p.465
Dikpati M., Charbonneau P., 1999, ApJ, 518, 508
Hatzes A. P., 1995, ApJ, 451, 784
Hoyng P., 1991, In: Schmelz J. T., Brown J. C. eds., The Sun: A Laboratory for Astrophysics, Scotland: Kluwer Press, p.99
Ivanova T. S., Ruzmaikin A. A., 1985, Astron. Nachr., 306, 177
Jetsu L., Pelt J., Tuominen I., 1993, A&A, 278, 449
Joncour I., Bertout C., Menard F., 1994, A&A, 285, L25
Kitchatinov L. L., 2002, A&A, 394, 1135
Küker M., Rüdiger G., 1999, A&A, 346, 922
Küker M., Rüdiger G., Schultz M., 2001, A&A, 374, 301
Krause F., Rädler K. H., 1980, Mean-field Magnetohydrodynamics and Dynamo Theory., Oxford: Pergamon Press
Krause F., Meinel R., 1988, Geophys. Astrophys. Fluid Dyn., 43, 95
Moffatt H. K., 1978, Manetic Field Generation in Electrical Conducting Fluids, Cambridge Univ.
Moss D., Tuominen I., Brandenburg A., 1991, A&A, 245, 129
Ossendrijver M., Stix M., Brandenburg A., 2001, A&A, 376, 713
Ossendrijver M., 2003, A&ARv., 11, 287
Parker E. N., 2001, ChJAA, 1, 99
Piskunov N. E., Tuominen I., Vilhu O., 1990, A&A, 230, 363
Rädler K. H., Bräuer H.,J., 1987, Astron. Nachr., 308, 101
Rice J. B., Strassmeier K. G., 1996, A&A, 316, 164
Rice J. B., Strassmeier K. G., 1998, A&A, 336, 792
Rüdiger G., Elstner D., Ossendrijver M., 2003, A&A, 406, 15
Rüdiger G., Elstner D., 1994, A&A, 282, 46
Schubert G., Zhang K., 2000, ApJ, 532, L149
Schubert G., Zhang K., 2001, ApJ, 557, 930
Steenbeck M., Krause F., 1969, Astron. Nachr., 291, 271
Zhang K., Liao X., 2003, ChJAA, 3, 12